Supporting Information

Tanaka et al. 10.1073/pnas.1102153108

SI Materials and Methods

Animals. Fertilized chicken and softshelled turtle (*Pelodiscus sinensis japonicus*) eggs were obtained from local hatcheries (chicken; Takeuchi Hatchery and turtle; Tujimura Hatchery). Chicken and turtle eggs were incubated under high humidity at 38 °C and 30 °C, respectively, until surgical manipulation. Chicken embryos (1) and turtle embryos (2) were staged as described previously. Common marmosets have been maintained in cages measuring 50 × 60 × 70 cm in our laboratory at the Central Institute for Experimental Animals (CIEA) since 1975. In marmosets, ovulation day was determined by the serum progesterone level exceeding 10 ng/mL and recorded as embryonic day 0 (E0). Breeder/host C57BL/6NCrSlc mice and ICR mice were obtained from SLC Japan. Embryonic mouse donor tissue was obtained by crossing ICR WT female mice with homozygous GFP-expressing C57BL/6-Tg(CAG-EGFP)C14-Y01-FM131Osb male mice (3). In mice, the day that a vaginal plug was detected at 12:00 PM was recorded as E0.5, and E19.5 was counted as postnatal day 0 (P0). All experiments were approved by the institutional animal care and use committee and were performed in accordance with institutional guidelines for animal experiments at Keio University and CIEA.

Donor Tissue Dissection and Labeling. To obtain E13.5 GFP-expressing mouse medial ganglionic eminence (MGE) cells, the approximate ventricular and subventricular zones of the MGE were dissected in chilled HBSS devoid of calcium and magnesium (Sigma). MGE explants were mechanically dissociated into a single-cell suspension in Leibovitz's L-15 medium (Invitrogen) containing DNase I (100 μg/mL; Sigma) by repeated pipetting using a pipette with a 200-μL tip (15–25 times). After centrifugation (5 min at 800 × *g*), the cell pellet was suspended in chilled Cell Banker cell conservation medium (BCL-1; Wako Pure Chemical) and stored at −80 °C or in liquid nitrogen until used. This nerve cell cryopreservation technique (4) increased the efficiency of donor cell preparation. Although it could be argued that this procedure impaired the migratory property of the cells, we think that it is unlikely to have occurred, because the distribution of cryopreserved GFP-expressing mouse MGE cells was very similar to that of noncryopreserved mouse MGE cells (5–7). To obtain chicken, turtle, and marmoset MGE cells, we used E5.5–E7.5 chicken embryos (approximately corresponding to Hamburger and Hamilton stages 27–31) (1), E16 turtle embryos (approximately corresponding to Tokita and Kuratani stage 15) (2), and E86–E96 marmoset embryos, respectively. Single-cell suspensions were prepared in the same manner as described above in regard to mouse cells. The MGE region of chicken, turtle, and marmoset brains as well as mouse brains was defined as the dorsal eminence within the Nkx2.1-expressing region of the subpallium (8). Sauropsid (chicken and turtle) cells and marmoset cells were pelleted by centrifugation and transfected with pCAG-mCherry (9, 10) using a chicken nucleofector kit (Amaxa Biosystems) and mouse nucleofector kit (Amaxa Biosystems), respectively, according to the manufacturer's instructions with some minor modifications. Because the number of turtle MGE cells obtained from ∼40 embryos per dissection procedure was too small to be labeled with Amaxa nucleofector, the turtle MGE cells were cryopreserved in the same manner as the mouse MGE described above in a single tube, and thawed turtle cells from three to four cryopreserved tubes were used for transfection. Immediately after transfection, cell suspensions were diluted in Leibovitz's L-15 medium and pelleted by centrifugation. Cryopreserved GFP-expressing mouse cells were thawed at 37 °C, and then, they were immediately diluted in L-15 medium and pelleted by centrifugation. The transfected chicken, turtle, or marmoset cells were mixed well with GFP-expressing mouse cells in L-15 medium containing 100 μg/mL DNase I and pelleted by centrifugation. Cell suspensions (∼10^6 cells/μL in L-15 medium containing 100 μg/mL DNase I) were kept on ice until used. To examine the behavior of chicken dorsal ventricular ridge (DVR) cells, the DVR region was dissected from E6.5 chicken embryos, dissociated into a single-cell suspension, and transfected with pCAG-mCherry in the same manner as the cells from the MGE region described above. To label mouse MGE cells born at a certain developmental stage, an IdU (Sigma) solution (10 mg/mL), prepared by a diluting IdU dimethyl sulfoxide solution (50 mg/mL in dimethyl sulfoxide) with distilled water, or a BrdU (Sigma) solution (10 mg/mL in PBS) was injected into the abdominal cavity of pregnant mice at a dose of 50 μg IdU/g body weight or 50 μg BrdU/g body weight, respectively, and embryos were collected ∼12 h later. To label chicken MGE cells born at a certain developmental stage, 100 μL IdU solution (10 mg/mL) or BrdU solution (10 mg/mL) were injected directly through the shell into the egg, and the hole was sealed with an adhesive bandage. After the injection, incubation of the eggs was continue under high humidity at 38 °C, and embryos were collected ∼6 h later.

Cell Transplantation. The donor cell suspensions were front-loaded into beveled glass micropipettes (50- to 75-μm caliber at the tip, GD-1; Narishige). For injection into the MGE in utero, pregnant C57BL/6NCrSlc mice were deeply anesthetized with sodium pentobarbital (100 mg/kg body weight, Nembutal; Abbott), and laparotomy was performed to expose their uteri. Approximately 3×10^4 cells (∼0.03 μL) were injected into the MGE of the left hemisphere of each embryo in utero under a stereomicroscope. The *x* and *y* coordinates of the injection sites were estimated from the surface anatomy (Fig. S2), and the *z* coordinate of the injection sites was ∼0.9 mm below the skin surface. Cell flow within the pipette during the injection was confirmed visually during every injection. After the injection procedure, the embryos were repositioned into the abdominal cavity, and the abdominal wall and skin were sutured closed. For injection into the cortical plate (CP) of the medial prefrontal cortex (mPFC) of neonates, P0 host mice were anesthetized by chilling on ice and then fixed in position under a stereomicroscope. Approximately 10^5 cells (∼0.1 μL) were transcranially injected into the mPFC of each hemisphere (total = 2×10^5 cells per animal). The *x* and *y* coordinates of the injection sites were estimated from the surface anatomy: the rostrocaudal level of the injection site was one-fourth of the distance from the rostrocaudal level of the center of the eye to the rostrocaudal level of the lambdoid suture. The mediolateral level of the injection site was one-eighth of the distance from the mediolateral level of the center of the eye to the midline. The injection site was defined as the point of intersection between a line passing through the rostrocaudal level of the injection site and a line passing through the mediolateral level of the injection site in each hemisphere. The *z* coordinate of the injection sites was ∼0.9 mm below the skin surface. Immediately after the injections, the recipient mice were placed on a warm surface until they became active, and then, they were returned to their mothers until they reached weaning age (4 wk).

Immunohistochemistry. Chicken, turtle, and mouse embryos were decapitated, and their brains were fixed in 4% paraformaldehyde

(PFA) in PBS (0.1 M, pH 7.4) at 4 °C for 6 h to overnight and then washed with PBS. Marmoset embryos were transcardially perfused with 4% PFA in PBS, and their brains were removed, postfixed at 4 °C for 2 h to overnight in the same fixative, and then washed with PBS. Postnatal mice were deeply anesthetized with diethyl ether and then perfused transcardially with 4% PFA in PBS. Their brains were removed and postfixed for 2 h to overnight in the same fixative at 4 °C. Brains were cryoprotected in 30% sucrose in PBS at 4 °C for cryosectioning. Coronal sections were cut with a vibrating-blade microtome (50–100 μm, VT-1000; Leica Microsystems) or a frozen sliding microtome (8–15 μm, CM3050 M; Leica Microsystems). For immunostaining without sectioning, the medial cortical walls of the telencephalic hemispheres from chicken, turtle, mouse, and marmoset brains were removed. The hemispheres were incubated in methanol with 0.3% hydrogen peroxide for 30 min at room temperature (RT) and then washed with PBS. Sections and hemispheres were incubated in PBS with 0.3% Triton X-100 and 5% normal donkey serum (NDS) for 1–2 h at RT and then for 2 h to 2 d at RT in the primary antibody diluted in PBS with 0.3% Triton X-100 and 1% NDS. The primary antibodies used were rabbit anti–TTF-1 (Nkx2-1, 1:500 to 1:1,000; Biopat), chicken anti-GFP (1:500; Abcam), goat biotin-conjugated anti-GFP (1:2,000; Rockland), rabbit anti-dsRed (1:300; Clontech), mouse anti-mCherry (1:200; Clontech), mouse anti-BrdU (which recognizes both BrdU and IdU, 1:50; BD), rat anti-BrdU (which recognizes BrdU but not IdU, 1:200; abcam), mouse antiparvalbumin (1:1,000; Sigma), and rat antisomatostatin (1:50 to 1:100; Millipore). Some sections were incubated for 3 h at RT in Alexa488-avidin (1:400; Molecular Probes) diluted in PBS, and others were incubated for 1 h to 1 d at RT in a secondary antibody diluted in 1% NDS in PBS. The secondary antibodies used were donkey FITC-, DyLight549-, or TRITC-conjugated anti-rabbit IgG, donkey DyLight488-conjugated anti-chicken IgY, donkey DyLight549- or Cy5-conjugated anti-mouse IgG, donkey TRITC- or Cy5-conjugated anti-rat IgG (all at 1:100), donkey biotinylated anti-rabbit IgG (1:2,000, all from Jackson ImmunoResearch), and Alexa555-conjugated goat anti-rabbit IgG (1:750; Molecular Probes). Hemispheres were incubated with avidin-biotin peroxidase complex (1:50, Vectastain ABC Elite kit; Vector Laboratories) in PBS for 1 h, washed with Tris-buffered saline (TBS; pH 7.5), and then incubated in 0.05% 3,3′-diaminobenzidine tetrahydrochloride (DAB) in TBS for 30 min. Color was developed in 0.05% DAB with 0.025% hydrogen peroxide in TBS. For nuclear staining, sections were incubated in 1% DAPI (Sigma) in PBS for 10–30 min at RT. For staining of BrdU and IdU, sections were first processed for GFP immunohistochemistry, and after incubating them in citrate buffer (0.01 M, pH 6.0) for 10 min at 99 °C and 30 min at RT, they were incubated in hydrogen chloride solution (4 M) for 15 min at RT and processed for BrdU and IdU staining. Images were captured with a CCD camera (VB-7010; Keyence) attached to an epifluorescence microscope (BX60; Olympus or MZFL3; Leica) or with a confocal microscope (FV1000; Olympus).

Quantification of Transplanted Cells. All transplanted brains in which the distribution of GFP-expressing mouse MGE cells was abnormal compared with reports in the literatures (5–7) were excluded from the analyses.

To quantify the rostrocaudal dispersion of the labeled cells, three slices from each brain were examined. First, the slice that contained the largest cluster of transplanted cells was designated the middle-level slice (middle slice). Then, a slice 350 μm rostral to the middle slice and a slice 350 μm caudal to the middle slice were designated the rostral-level slice (rostral slice) and the caudal-level slice (caudal slice), respectively. In the rostral slice, all labeled cells found ventromedial to a line passing through the corticostriatal boundary at a 45° angle and dorsolateral to a line passing through the sulcus between the lateral ganglionic eminence and septum at a 45° angle were included in the analysis. In the middle slice, all labeled cells found ventromedial to the 45° angle line through the corticostriatal boundary and dorsolateral to the 45° angle line through the dorsal edge of the cluster of transplanted cells were included in the analysis. In the caudal slice, all labeled cells found ventromedial to the 45° angle line through the corticostriatal boundary and dorsolateral to the 45° angle line through the sulcus between the caudal ganglionic eminence and thalamus were included in the analysis.

To quantify the zonal distribution of the labeled cells, all labeled cells found ventrolateral to a vertical line drawn through the dorsal edge of the cortex and mediodorsal to the corticostriatal boundary were included in the analysis. For the analysis of embryonic and neonatal brains, coronal sections were obtained from the rostral end to the caudal end of the ganglionic eminence, and for the analysis of P7 brains, coronal sections were obtained from the rostral end to the caudal end of the corpus callosum. The cortical zones were determined based on the density and orientation of the nuclei labeled by DAPI.

To quantify the overall distribution of labeled cells in the archicortex, paleocortex, and neocortex, the ratio of the number of labeled cells in the gray matter of the hippocampus (archicortex) or piriform cortex (paleocortex) to the number of labeled cells in the gray matter of the barrel field of the primary somatosensory area (neocortex) (11) were analyzed.

To quantify expression of any of the markers in transplanted labeled cells, all pallial labeled cells found ventrolateral to the hippocampus and dorsomedial to the granular insular cortex in the rostral region or found ventrolateral to the hippocampus and dorsomedial to the entorhinal cortex in the caudal region were included in the analysis. Coronal sections were obtained from the rostral end of the corpus callosum to the point at which the hippocampus reached the ventral end of the telencephalon caudally. The labeled transplanted cells were examined for marker expression through the ×60 objective of a confocal microscope (FV1000; Olympus).

To quantify the survival rate of chicken MGE cells injected directly into the CP of the neonatal mPFC compared with transplanted mouse MGE cells, the ratio of the number of mCherry-expressing chicken MGE cells to the number of GFP-expressing mouse MGE cells within the prelimbic cortex (11) was calculated at 2, 12, and 24 wk after transplantation.

Statistical Analysis. All data were analyzed by the Mann–Whitney *u* test. A P value < 0.05 was considered statistically significant. All tests were two-tailed. All data were expressed as the mean ± SEM.

SI Discussion

Phylogenetic Origin of the Competency of MGE Cells to Migrate Within the Mammalian Neocortex. As for the competency of MGE cells to migrate tangentially through the neocortical subventricular zone/intermediate zone (SVZ/IZ) and the weak competency to enter neocortical layers 5 and 6 (Fig. S8*B*), two phylogenetic origins are possible. The first is that the MGE cells in the ancestor of amniotes had the competencies; the second is that the MGE cells in the ancestor of amniotes did not have the competencies, but they were established independently in mammals and sauropsids after phylogenetic divergence. The first possibility is more plausible, because it requires only a single evolutionary change (a gain of the competencies in the ancestor of amniotes), whereas the second requires at least two (a gain of the competencies in the ancestor of mammals and the ancestor of sauropsids). We, therefore, propose that the competency of MGE cells to migrate tangentially through the neocortical SVZ and their weak competency to enter neocortical layers 5 and 6 had already been established in the ancestor of amniotes (Fig. S8*C*). In view of the fact that the neocortical SVZ emerged in the ancestor of eutherians 148 MYA (12, 13), the MGE cells of the ancestor of amniotes that lived 310

MYA (14, 15) already had proper responsiveness to guidance cues to migrate in the neocortical SVZ that emerged 162 million y later. Thus, the MGE cells of the ancestor of amniotes were preadapted to the mammalian neocortical SVZ in regard to their tangential migration, providing empirical evidence for the evolutionary concept of preadaptation (16) in the developing brain.

As for the phylogenetic origin of the competency of MGE cells to enter the neocortical CP, we speculate that there are two possible explanations. The first is that the competency was already established in the common ancestor of the mouse and marmoset, possibly in the ancestor of mammals, because many interneurons have been observed even in the neocortical CP of a monotreme (17). The second is that the MGE cells in the ancestor of amniotes possessed the competency, but the competency was lost between the ancestor of amniotes (310 MYA) and the ancestor of archosauromorphs, the common ancestor of chickens and turtles (240–260 MYA) (14, 15, 18). The first possibility seems more plausible, because it requires only a single evolutionary change (a gain of the competencies in the ancestor of mammals), whereas the second requires at least two evolutionary changes (a gain of the competencies in the ancestor of mammals and its loss in the ancestor of archosauromorphs). We, therefore, think that the competency of MGE cells to enter the neocortical CP, especially layers 2–4, and the MZ was established in the ancestor of mammals (Fig. S8*C*).

Distribution and Dispersion of Interneurons Within the Neocortical MZ. Most sauropsid MGE cells not only failed to enter the MZ during their migration but also failed to be distributed within the CP, especially in layers 2–4 (Fig. S8*B*), raising the possibility that the transient accumulation and dispersion of interneurons within the MZ during their migration (9, 19–22) may be required for their final proper distribution within the CP, especially in layers 2–4. Consistent with this possibility, disrupted distribution of a certain subset of interneurons within the CP, especially within the upper end of layers 2 and 3, has been observed in Dlx5/6-CreER:Cxcr4-floxed mice, in which interneurons fail to distribute within the MZ but do distribute in the SVZ during their migration (23). Thus, the gain of migratory competency within the neocortical MZ by MGE cells during mammalian evolution (Fig. S8*C*) may have been the critical step in striking the proper balance between excitation and inhibition within layers 2–4.

1. Hamburger V, Hamilton HL (1951) A series of normal stages in the development of the chick embryo. *J Morphol* 88:49–92.
2. Tokita M, Kuratani S (2001) Normal embryonic stages of the Chinese softshelled turtle Pelodiscus sinensis (Trionychidae). *Zoolog Sci* 18:705–715.
3. Okabe M, Ikawa M, Kominami K, Nakanishi T, Nishimune Y (1997) 'Green mice' as a source of ubiquitous green cells. *FEBS Lett* 407:313–319.
4. Paynter SJ (2008) Principles and practical issues for cryopreservation of nerve cells. *Brain Res Bull* 75:1–14.
5. Nery S, Fishell G, Corbin JG (2002) The caudal ganglionic eminence is a source of distinct cortical and subcortical cell populations. *Nat Neurosci* 5:1279–1287.
6. Wichterle H, Turnbull DH, Nery S, Fishell G, Alvarez-Buylla A (2001) In utero fate mapping reveals distinct migratory pathways and fates of neurons born in the mammalian basal forebrain. *Development* 128:3759–3771.
7. Pla R, Borrell V, Flames N, Marín O (2006) Layer acquisition by cortical GABAergic interneurons is independent of Reelin signaling. *J Neurosci* 26:6924–6934.
8. Flames N, et al. (2007) Delineation of multiple subpallial progenitor domains by the combinatorial expression of transcriptional codes. *J Neurosci* 27:9682–9695.
9. Tanaka DH, et al. (2009) Random walk behavior of migrating cortical interneurons in the marginal zone: Time-lapse analysis in flat-mount cortex. *J Neurosci* 29:1300–1311.
10. Niwa H, Yamamura K, Miyazaki J (1991) Efficient selection for high-expression transfectants with a novel eukaryotic vector. *Gene* 108:193–199.
11. Franklin KBJ, Paxinos G (2008) *The Mouse Brain in Stereotaxic Coordinates* (Academic, New York), 3rd Ed.
12. Puzzolo E, Mallamaci A (2010) Cortico-cerebral histogenesis in the opossum Monodelphis domestica: Generation of a hexalaminar neocortex in the absence of a basal proliferative compartment. *Neural Dev* 5:8.
13. Bininda-Emonds OR, et al. (2007) The delayed rise of present-day mammals. *Nature* 446:507–512.
14. Benton MJ (1990) Phylogeny of the major tetrapod groups: Morphological data and divergence dates. *J Mol Evol* 30:409–424.
15. Kumazawa Y, Nishida M (1999) Complete mitochondrial DNA sequences of the green turtle and blue-tailed mole skink: Statistical evidence for archosaurian affinity of turtles. *Mol Biol Evol* 16:784–792.
16. Bock WJ (1959) Preadaptation and multiple evolutionary pathways. *Evolution* 13: 194–211.
17. Hassiotis M, Paxinos G, Ashwell KW (2005) Cyto- and chemoarchitecture of the cerebral cortex of an echidna (Tachyglossus aculeatus). II. Laminar organization and synaptic density. *J Comp Neurol* 482:94–122.
18. Iwabe N, et al. (2005) Sister group relationship of turtles to the bird-crocodilian clade revealed by nuclear DNA-coded proteins. *Mol Biol Evol* 22:810–813.
19. Ang ES, Jr., Haydar TF, Gluncic V, Rakic P (2003) Four-dimensional migratory coordinates of GABAergic interneurons in the developing mouse cortex. *J Neurosci* 23:5805–5815.
20. Tanaka D, Nakaya Y, Yanagawa Y, Obata K, Murakami F (2003) Multimodal tangential migration of neocortical GABAergic neurons independent of GPI-anchored proteins. *Development* 130:5803–5813.
21. Tanaka DH, Maekawa K, Yanagawa Y, Obata K, Murakami F (2006) Multidirectional and multizonal tangential migration of GABAergic interneurons in the developing cerebral cortex. *Development* 133:2167–2176.
22. Yokota Y, et al. (2007) Radial glial dependent and independent dynamics of interneuronal migration in the developing cerebral cortex. *PLoS One* 2:e794.
23. Tanaka DH, et al. (2010) CXCR4 is required for proper regional and laminar distribution of cortical somatostatin-, calretinin-, and neuropeptide Y-expressing GABAergic interneurons. *Cereb Cortex* 20:2810–2817.

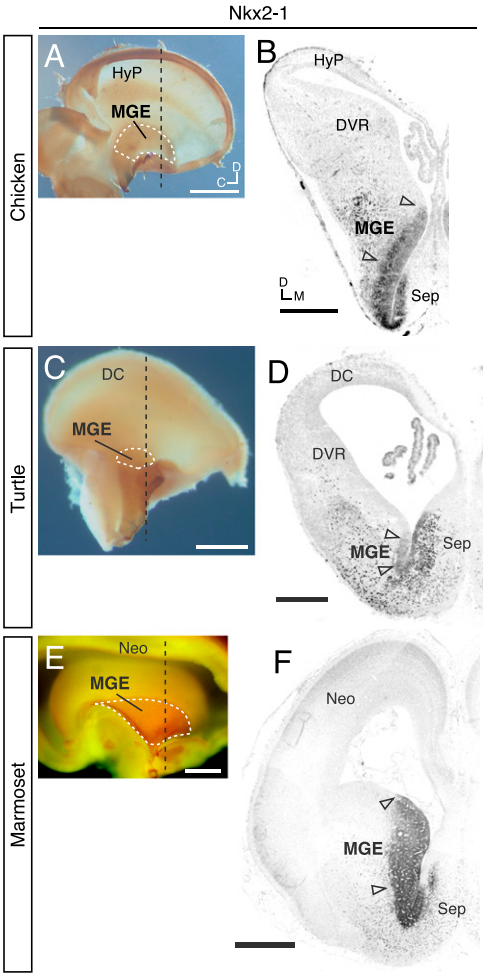

Fig. S1. Expression of Nkx2-1 in embryonic chicken, turtle, and marmoset forebrains. (*A*, *C*, and *E*) Medial view of Nkx2-1 expression (brown) in the left hemisphere of E6.5 chicken (*A*), E16 turtle (*C*), or E92 marmoset (*E*) embryos. The medial wall of the pallium was removed before immunostaining. The region outlined by the broken white line is approximately the MGE region that was dissected for transplantation. (*B*, *D*, and *F*) Nkx2-1 expression (black) in a coronal section of E6.5 chicken (*B*), E16 turtle (*D*), and E91 marmoset (*F*) brain through the rostrocaudal level that is approximately indicated by the broken gray line in *A*, *C*, and *E*, respectively. Regions sandwiched between arrowheads are approximately the MGE regions that were dissected for transplantation. MGE, medial ganglionic eminence; HyP, hyperpallium; DVR, dorsal ventricular ridge; Sep, septum; DC, dorsal cortex; Neo, neocortex; C, caudal; D, dorsal; M, medial. (Scale bars: *A*, *E*, and *F*, 1 mm; *B*, 200 μm; *C*, 500 μm; *D*, 300 μm.)

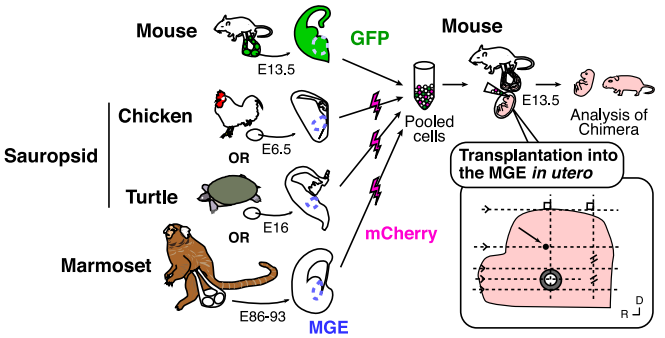

Fig. S2. Schema of the experimental design. The MGE was dissected from E13.5 mouse embryos expressing GFP and E6.5 chicken, E16 turtle, and E86–E93 marmoset embryos, and the chicken, turtle, and marmoset MGE cells were labeled with mCherry by electroporation. Pooled donor cells were then injected into the MGE of E13.5 host embryos in utero. A balloon shows the schema of *x* and *y* coordinates of the injection site (black dot indicated by the arrow) on a view of the left side of the head of a recipient mouse embryo. The positions of the *x* and *y* coordinates of the injection sites were estimated on the basis of the surface anatomy. The rostrocaudal level of the injection site was slightly rostral to the center of the left eye. The dorsoventral level of the injection site was rostral to the dorsal edge of the eye for a diameter of the eye. The *z* coordinate of the injection sites was ~0.9 mm below the skin surface. Only the left hemisphere was injected. The host brains were analyzed at later stages. D, dorsal; R, rostral.

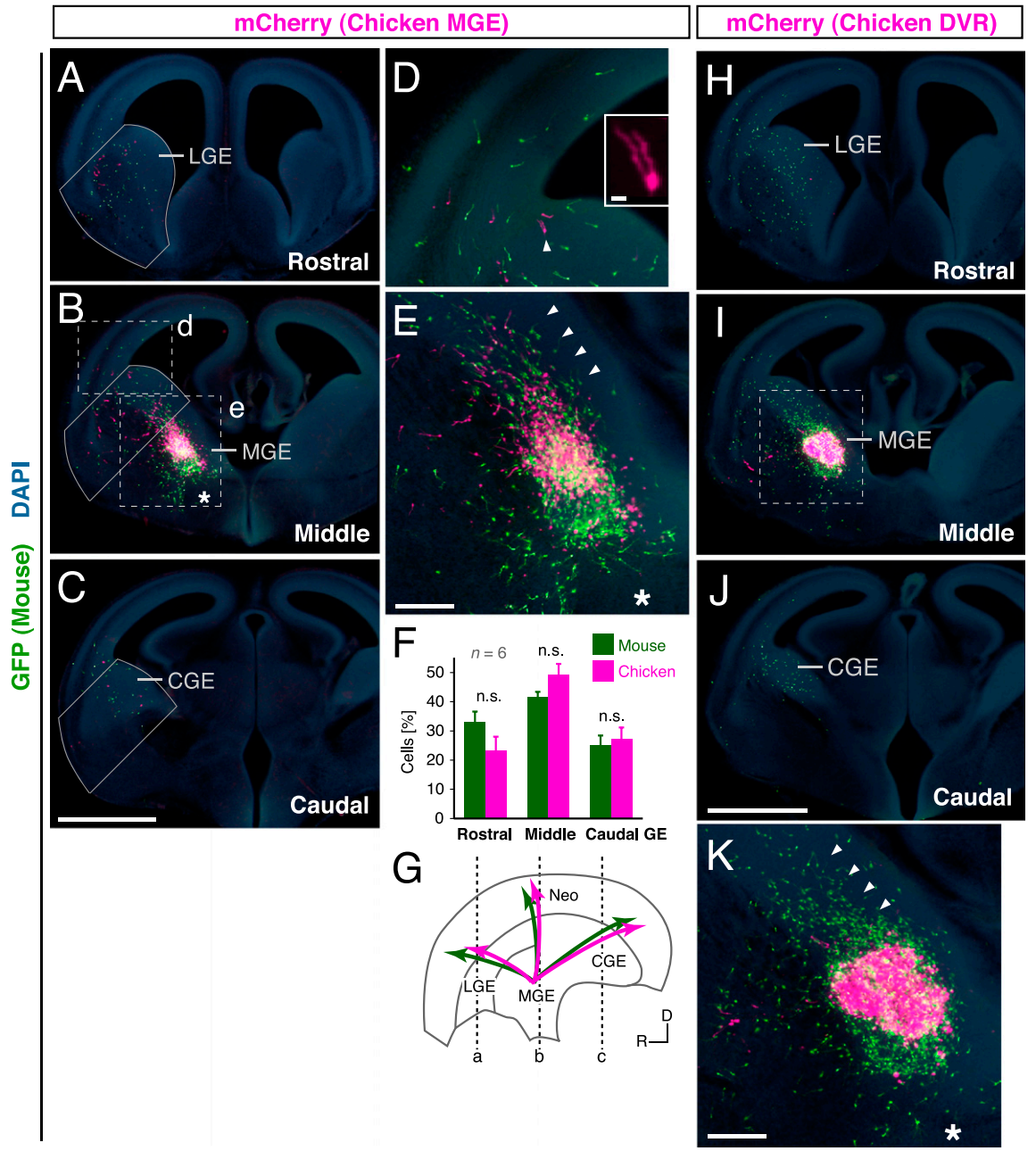

Fig. S3. Chicken MGE cells but not DVR cells dispersed dorsally in the mouse telencephalon, the same as mouse MGE cells did. (*A–C*) Distribution of GFP-expressing mouse MGE cells (green) and mCherry-expressing chicken MGE cells (magenta) in a coronal section through the rostral level (*A*), middle level (*B*), and caudal level (*C*) of a host forebrain at E15.5. Transplantation with chicken MGE cells was performed as illustrated in Fig. S2. (*D*) Enlarged view of boxed region d in *B*. *Inset* shows an enlarged view of the mCherry-expressing cell indicated by the arrowhead. (*E*) Enlarged view of boxed region e in *B*. Most of both GFP-expressing and mCherry-expressing cells migrated dorsolaterally (arrowheads), and few migrated ventromedially (asterisk). (*F*) Quantification of the distribution of GFP-expressing mouse MGE cells and mCherry-expressing chicken MGE cells along the rostrocaudal axis. The percentages of GFP-expressing cells and mCherry-expressing cells in the rostral, middle, or caudal regions enclosed within lines in *A–C*, respectively, were analyzed (mean ± SEM; $n = 6$ brains, 898 GFP-expressing and 1,168 mCherry-expressing cells). There were no statistically significant differences between the percentage of GFP-expressing cells and mCherry-expressing cells at the rostral level ($P = 0.093$, Mann–Whitney U test), the middle level ($P = 0.064$), and the caudal level ($P = 1$). (*G*) Schema of a medial view of a right hemisphere showing the approximate rostral level a (*A*), middle level b (*B*), and caudal level c (*C*) analyzed and the presumptive migratory pathways of mouse MGE cells (green arrows) and chicken MGE cells (magenta arrows) from the mouse MGE region. (*H–J*) Distribution of GFP-expressing mouse MGE cells (green) and mCherry-expressing chicken DVR cells (magenta) in a coronal section through the rostral (*H*), middle (*I*), and caudal levels (*J*) of a host forebrain at E15.5. Transplantation was performed as illustrated in Fig. S2, but chicken DVR cells were used instead of chicken MGE cells. (*K*) Enlarged view of the boxed region in *I*. The GFP-expressing mouse MGE cells migrated dorsolaterally (arrowheads) and few migrated ventrally (asterisk), whereas most mCherry-expressing chicken DVR cells did not migrate in either direction. Similar results were obtained in all host brains analyzed ($n = 6$ brains). LGE, lateral ganglionic eminence; MGE, medial ganglionic eminence; CGE, caudal ganglionic eminence; Neo, neocortex; DVR, dorsal ventricular ridge; R, rostral; D, dorsal. (Scale bars: *A–C* and *H–J*, 1 mm; *D*, *E*, and *K*, 200 μm; *D Inset*, 10 μm.)

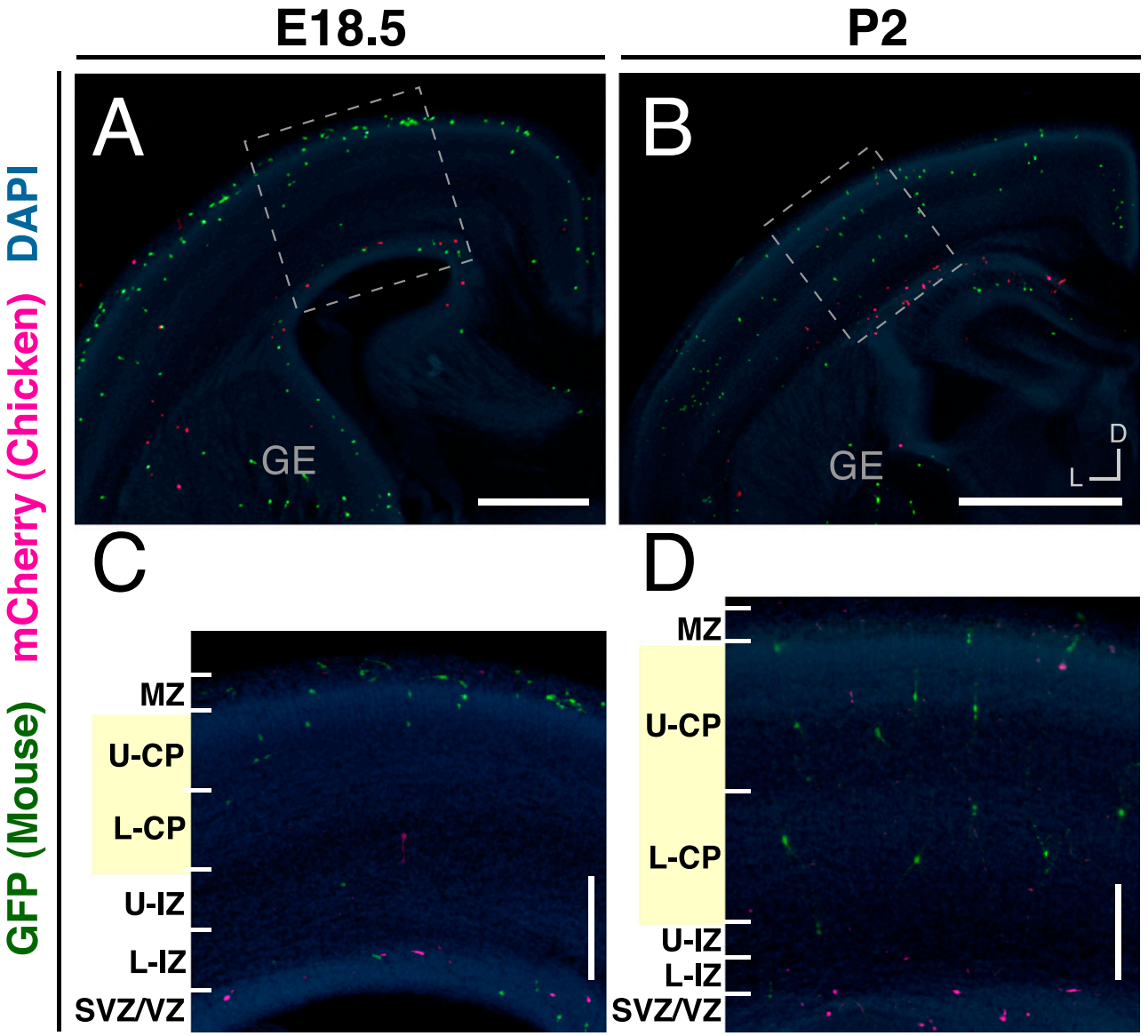

Fig. S4. Most chicken MGE cells migrated medially through the neocortical SVZ/IZ, the same as mouse MGE cells did, but failed to enter the CP/MZ. (*A* and *B*) Distribution of GFP-expressing mouse MGE cells (green) and mCherry-expressing chicken MGE cells (magenta) in coronal sections through the middle level along the rostrocaudal axis of the host forebrain at E18.5 (*A*) and P2 (*B*). Transplantation with chicken MGE cells was performed as illustrated in Fig. S2. (*C* and *D*) Enlarged views of the boxed regions in *A* and *B*. GE, ganglionic eminence; L, lateral; D, dorsal. (Scale bars: *A*, 500 μm; *B*, 1 mm; *C* and *D*, 200 μm.)

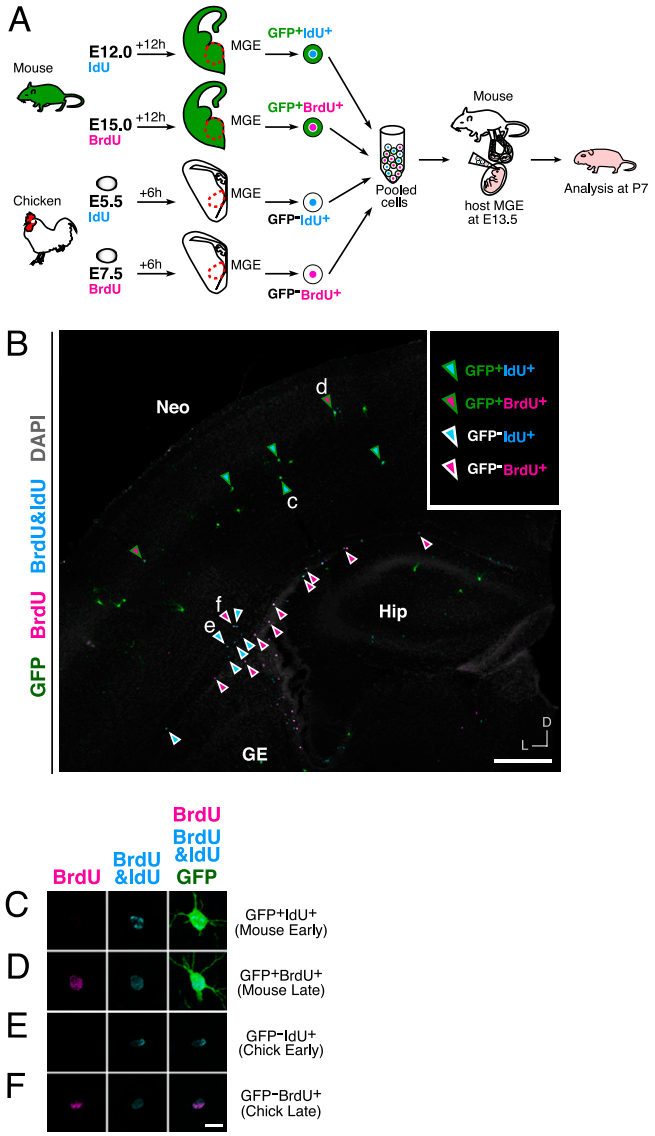

Fig. S5. A majority of the chicken MGE cells failed to enter the CP/MZ regardless of their birthdates. (*A*) Schema of the experimental design. GFP-expressing mouse MGE cells were labeled with IdU at E12.0, and GFP-expressing mouse MGE cells from other pregnant mice were labeled with BrdU at E15.0. The labeled mouse MGE cells were dissected and dissociated 12 h later. Similarly, chicken MGE cells were labeled with IdU at E5.5, and chicken MGE cells from other eggs were labeled with BrdU at E7.5. The labeled chicken MGE cells were dissected and dissociated 6 h later. The four differentially labeled cells were pooled and simultaneously transplanted into a mouse MGE at E13.5 in utero, and the hosts were analyzed at P7. (*B*) Distribution of the GFP-expressing cells (green), BrdU-positive cells (magenta), and BrdU and/or IdU-postive cells (cyan) in the host neocortex at P7. Arrowheads outlined in green represent GFP-positive IdU-positive cells when filled with cyan and GFP-positive BrdU-positive cells when filled with magenta. Similarly, arrowheads outlined in white represent GFP-negative IdU-positive cells when filled with cyan and GFP-negative BrdU-positive cells when filled with magenta. (*C*–*F*) Enlarged views of cells labeled c–f in *B*. Neo, neocortex; Hip, hippocampus; GE, ganglionic eminence; L, lateral; D, dorsal. (Scale bars: *B*, 500 μm; *C*–*F*, 10 μm.)

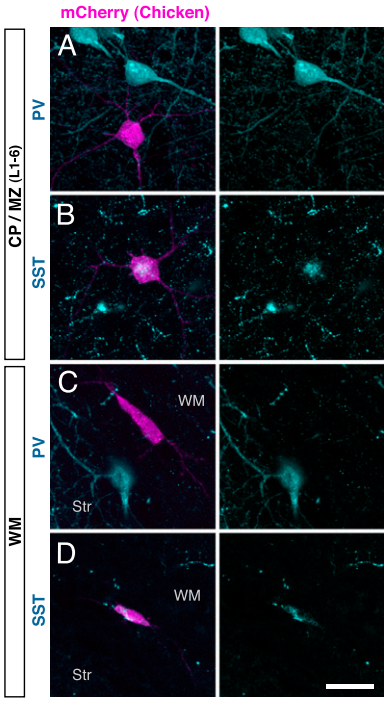

Fig. S6. Expression of interneuron subtype markers in chicken MGE cells within the juvenile neocortex. Expression of parvalbumin (light blue; *A* and *C*) and somatostatin (light blue; *B* and *D*) in mCherry-expressing chicken MGE cells (magenta) distributed in the CP (layers 2–6) and MZ (layer 1; *A* and *B*) and in white matter (*C* and *D*) at P23. Transplantation with chicken MGE cells was performed as illustrated in Fig. S2. WM, white matter; Str, striatum; PV, parvalbumin; SST, somatostatin. (Scale bar: 20 μm.)

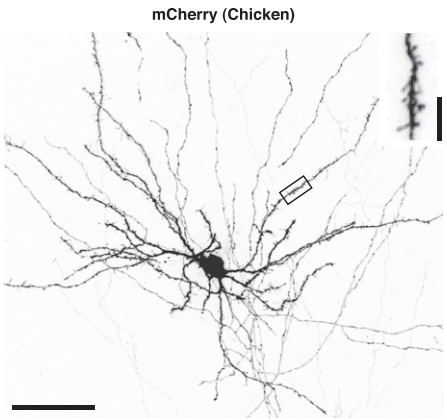

Fig. S7. The neocortical CP is essentially permissive in regard to the postmigratory development of chicken MGE cells. Representative morphology of mCherry-expressing chicken MGE cells within neocortical layers 2–4 at P23. Dorsal is to the brain surface. *Inset* shows an enlarged view of the boxed region. Transplantation with chicken MGE cells was performed as illustrated in Fig. S2. (Scale bars: 40 μm; *Inset*, 5 μm.)

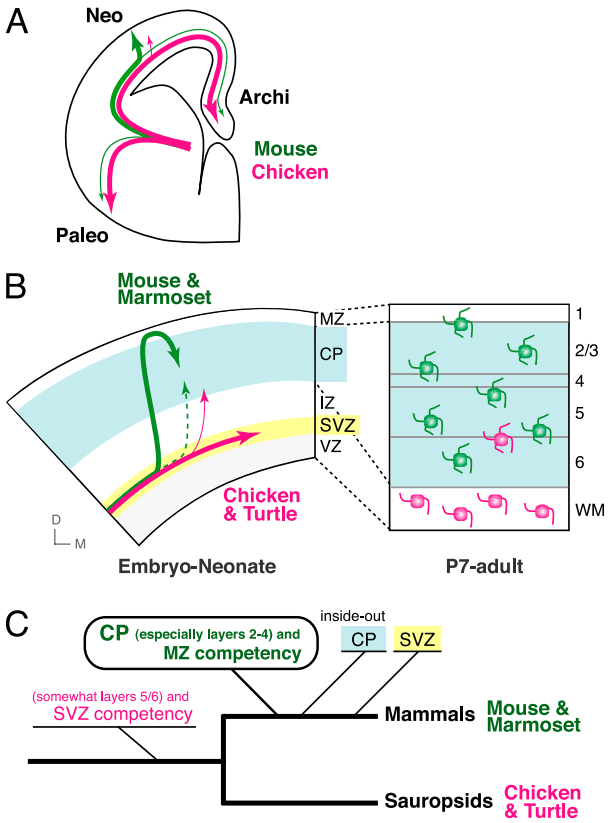

Fig. S8. The migratory competency of MGE cells to enter the neocortical CP/MZ seems to have been established in the ancestor of mammals. (*A*) Model of the ratios of mouse (green) and chicken (magenta) MGE cells that entered the gray matter of the mouse neocortex, archicortex, and paleocortex. Most mouse MGE cells entered the neocortex, and most chicken MGE cells entered the archicortex and paleocortex. (*B*) Model of the migratory pathways within the mouse neocortex of cells derived from mouse, marmoset, chicken, and turtle MGE. The MGE cells derived from the all species examined migrate tangentially through the mouse neocortical SVZ. The mammalian (mouse and marmoset) MGE cells subsequently entered the CP/MZ, but most sauropsid (chicken and turtle) MGE cells did not; they especially did not enter layers 2–4 within the CP and the MZ. (*C*) Model of the phylogenetic origins of the competencies of MGE-derived interneurons to migrate within the neocortex. The SVZ and inside-out CP of the dorsal pallium (the neocortex in mammals) are established in the ancestor of eutherians and a more primitive ancestor, respectively (1). Although the phylogenetic origin of the competencies of MGE cells to migrate in the SVZ and some competencies of MGE cells to enter layers 5 and 6 is the ancestor of amniotes, the competencies of MGE cells to enter the CP, especially layers 2–4, and the MZ are the ancestor of mammals. Additional discussion is in *SI Discussion*.

1. Puzzolo E, Mallamaci A (2010) Cortico-cerebral histogenesis in the opossum Monodelphis domestica: Generation of a hexalaminar neocortex in the absence of a basal proliferative compartment. *Neural Dev* 5:8.